American Mineralogist, Volume 71, pages 795–804, 1986

High-temperature crystal chemistry of dolomite

Richard J. Reeder
Department of Earth and Space Sciences, State University of New York at Stony Brook, Stony Brook, New York 11794
Steven A. Markgraf
Materials Research Laboratory, Pennsylvania State University, University Park, Pennsylvania 16802

Abstract

Structural parameters have been refined from X-ray intensity data for a stoichiometric dolomite single crystal at 24, 200, 400, and 600°C. Both a rigid-body model and a conventional anisotropic thermal model were used for refinements, yielding nearly identical values for temperature factors and residuals. This attests to the suitability of the rigid-body model over the temperature range studied.

Thermal expansion of a and c are similar to that of magnesite but markedly different from that of calcite. The Ca and Mg octahedra expand more rapidly than those in calcite and magnesite, respectively, and also differently. The Ca octahedron shows no increase in distortion with temperature as it does in calcite, and yet the Mg octahedron does, which contrasts with its behavior in magnesite. Rigid-body libration of the CO_3 group is intermediate in magnitude between that in calcite and magnesite, and neither rotation around the threefold axis nor out-of-plane tilting is dominant. Expansion of the libration-corrected C–O bond length is nearly identical to that in magnesite and substantially less than that in calcite.

No evidence of cation disorder is found throughout the temperature range studied.

Introduction

Over the past fifteen years, high-temperature crystal-structure investigations have been conducted for many rock-forming silicate and oxide minerals. More recently, interest in carbonate minerals has gained some attention. Reeder and Wenk (1983) refined structures of several dolomites quenched from temperatures between 1050 and 1200°C, obtaining information about cation disordering. Owing to re-ordering during quenching, they were unable to relate site distributions uniquely with temperature. Since intensity data were collected at room temperature, no evaluation of the effect of temperature on the structure was possible. Markgraf and Reeder (1985) recently refined the structures of calcite from data collected at several temperatures up to 800°C and of magnesite up to 500°C. We were specifically interested in the behavior of the CO_3 group in relation to thermal expansion and, in the case of calcite, in relation to proposed anion rotational disorder. The characterization of the CO_3 group using the rigid-body model proved to be very useful. The most significant finding was the rather different vibrational character in calcite than in magnesite. In the former, the dominant motion of the CO_3 group is a low-amplitude rotary oscillation around the threefold axis; in magnesite, it is more nearly a tilting out of the plane in which it lies.

The present study of dolomite can be viewed as an extension of our high-temperature work on calcite and magnesite. Our interest in understanding the high-temperature behavior of dolomite is quite varied. Dolomite, like calcite, can be described as a corner-linked structure of filled octahedra and nearly planar CO_3 groups. The lower symmetry of dolomite (space group $R\bar{3}$, compared with $R\bar{3}c$ for calcite) results from the alternating Ca and Mg layers and the slight rotation of the CO_3 groups which move the oxygens off the diad axes that exist in calcite. Since dolomite contains octahedra of both Ca and Mg, which as a first approximation are similar to those in calcite and magnesite, we have the opportunity to compare their relative behaviors in the same structure. Thermal expansion of dolomite is known to be positive for both a and c (Bayer, 1971), similar to magnesite but in contrast to calcite whose expansion along **a** is negative. The various factors influencing expansion in double carbonates has not previously been investigated.

In view of the role that thermal vibrations of the CO_3 group play in the single rhombohedral carbonates, it is desirable to understand their role in dolomite. The potential importance may be shown by two particular examples, one relating to the unusual strength-temperature relationship shown by dolomite. Higgs and Handin (1959) and more recently Barber et al. (1981) showed that critical resolved shear stress for all but one deformation mechanism increases with temperature in dolomite single crystals. Calcite single crystals show the more typical behavior of decreasing strength with temperature. Barber et al. at-

0003–004X/86/0506–0795$02.00

tributed this strength behavior in dolomite—particularly for c slip—to impedence of dislocation movement associated with thermal motion of the CO_3 group, which of course increases with temperature. At the time of their study there were no data describing thermal motions at high temperatures in either calcite or dolomite, when clearly a need existed.

As in the case of calcite, the question of possible CO_3-group rotational disorder in dolomite has been raised. Although Reeder and Nakajima (1982) and Reeder and Wenk (1983) have discussed some aspects pertaining to such anion disorder at high temperature, there is little evidence to support it. Changes in rigid-body motion parameters with temperature may provide an indication of premonitory behavior for such a transformation.

Our results reported here for single-crystal, high-temperature X-ray diffraction experiments on dolomite help to address these various considerations.

Experimental method

Specimen

The dolomite crystal used in this study was taken from a clear cleavage rhomb (measuring several centimeters in mean dimension) found in the magnesite deposits at Eugui in northern Spain. This sample is from the same cleavage rhomb that was used in earlier studies by Reeder and Wenk (1983) and Reeder and Nakajima (1982). Eugui dolomite has also been used for several other studies requiring good-quality single crystals, including the single-crystal deformation work of Barber et al. (1981). In their room-temperature refinement, Reeder and Wenk found the cation ordering to be ideal. Examination in the transmission electron microscope has shown that Eugui dolomite is homogeneous, with very low dislocation densities (cf. Barber et al., 1981; Reeder and Wenk, 1983).

The composition reported by Reeder and Wenk shows that it is nearly ideal—$Ca_{1.001}Mg_{0.987}Fe_{0.010}Mn_{0.002}(CO_3)_2$. The crystal used in this study has approximate dimensions of 240 × 235 × 95 μm. The crystal was mounted on a silica-glass fiber using Ceramobond 503 (Aremco Products, Inc.). It was put in a 0.5-mm silica capillary, which was then evacuated and sealed, and mounted in a standard goniometer head. Precession and Laue photography produced sharp spots and showed that it was a single crystal.

In situ heating

The crystal was heated using the heater described by Brown et al. (1973). The heater was precalibrated throughout the temperature range and was allowed to stabilize for roughly 2 h at each temperature prior to data collection. Error is estimated to be ±20°C. Decomposition of the sample eventually began at 700°C, not before we were able to center reflections for cell refinement, but precluding data collection for structure refinement. The onset of decomposition was signaled by the appearance of a white coating on the crystal surface. Based on the thermal decomposition curves determined by Graf and Goldsmith (1955), the partial pressure of CO_2 in the capillary at 600°C may have been of the order of 20 bars (this would presumably also be very nearly the total pressure). In order to prevent decomposition at 700°C, a CO_2 partial pressure in excess of 100 bars would have been needed. It is unlikely that the capillary used would have been able to retain such pressures.

Data collection

A automated Picker four-circle diffractometer operating with graphite-monochromated Mo$K\alpha$ radiation (λ = 0.7107 Å) was used to collect integrated intensities at 24, 200, 400, and 600°C. Roughly 530 diffraction intensities ($\sin\theta/\lambda < 0.81$) were collected at each temperature using the ω-2θ scan mode with a scan width of 2.0° + 0.7 tan θ and maintaining a constant precision of $\sigma_I/I = 0.01$, where σ_I is based on counting statistics. A standard intensity was collected every 20 reflections throughout each data set for the purposes of indicating crystal movement or decomposition.

Unit-cell parameters were refined at all temperatures for which intensity data were collected and also at 700°C. The least-squares refinement used 24 reflections ($0.50 < \sin\theta/\lambda < 0.65$), each of which was centered at positive and negative 2θ and then averaged.

Refinement details

Intensities were corrected for Lorentz and polarization effects and also absorption. For the latter, the crystal shape and orientation relative to the X-ray beam were modeled using D. K. Swanson's program BXL. The absorption corrections were calculated using a modified version of L. W. Finger's program ABSORB, yielding maximum and minimum transmission factors of 0.86 and 0.75, respectively ($\mu_{MoK\alpha}$ = 15 cm^{-1}). No absorption correction was made for the silica capillary. A reflection was considered unobserved when $I < 2\sigma_I$. Absorption-corrected data were symmetry-averaged, resulting in roughly 300 independent observations for each temperature. This resulted in an 18:1 ratio of independent observations to refined parameters.

Refinements were done using the least-squares program REFINE in the PROMETHEUS system (Zucker et al., 1983), which is a modified version of the program RFINE4 (Finger and Prince, 1975). It incorporates the rigid-body treatment (as implemented in RFINE4) by refining rigid-body parameters directly. Weights were assigned proportionally to $1/\sigma_F^2$, where σ_F is based on counting statistics. Starting parameters of Reeder and Wenk (1983) were used for the initial refinement. Final refinements used the isotropic extinction correction of Becker and Coppens (1975), assuming Type I behavior and a Lorentzian mosaic angular distribution. The refineable parameter **G**, for mosaic spread, ranged from 1.02(7) at 24°C to 0.77(6) at 400°C. Atomic scattering factor curves for neutral atoms and corrections for anomalous dispersion were taken from the *International Tables for X-ray Crystallography*, volume IV (Ibers and Hamilton, 1974).

In addition to the standard refinements using anisotropic temperature factors, we also carried out rigid-body refinements using the **T**, **L**, and **S** tensors (Schomaker and Trueblood, 1968) for the average thermal motion of the CO_3 group. In the previous work on calcite and magnesite, this method was found to be a useful description of the behavior of the CO_3 group. Also, the number of independent variable parameters is reduced by two, owing to the constraints of the model. Residuals for all refinements are given in Table 1. It should be noted that equivalent results were obtained with both models throughout the temperature range studied.

During the refinement of the data set collected at 600°C, site occupancies were allowed to vary to determine if any cation disorder could be detected. Occupancies refined to a state of essentially perfect order within estimated standard errors.

Results

Unit-cell parameters are reported in Table 2 and are shown in Figures 1 and 2. The room temperature values

Table 1. Data collection and refinement information for dolomite at several temperatures

TEMP (°C)	Total No.Obs.	No. Ind.Obs.	Anisotropic R*	Anisotropic R_w**	Anisotropic S***	Rigid-body R	Rigid-body R_w	Rigid-body S
24	532	312	0.022	0.032	2.11	0.023	0.033	2.18
200	530	307	0.021	0.030	2.03	0.022	0.032	2.12
400	533	303	0.023	0.030	1.99	0.024	0.032	2.11
600	536	303	0.022	0.030	1.88	0.024	0.032	2.01

* $R = \Sigma||F_o| - |F_c|| / \Sigma |F_o|$

** $R_w = [\Sigma w(|F_o| - |F_c|)^2 / \Sigma w|F_o|^2]^{1/2}$

*** Estimated standard deviation of unit weight observation.

compare reasonably well with those determined by Reeder and Wenk (1983), also for Eugui dolomite—$a = 4.8038(9)$ Å, $c = 16.006(4)$ Å. However, the present values compare more favorably with those determined independently on the same material using powder techniques. Reeder and Wenk reported cell parameters determined by Dr. H. Kroll with a Jagodzinski-Guinier camera—$a = 4.8073(5)$ Å, $c = 16.004(1)$ Å. Values determined by least-squares refinement of powder X-ray diffractometer data are given by Reeder and Sheppard (1984)—$a = 4.8078(6)$ Å; $c = 16.002(3)$ Å.

As we describe results of the influence of temperature on the various structural parameters, we will usually compare these with the corresponding behavior that we found for calcite and magnesite (Markgraf and Reeder, 1985). To facilitate this comparison we often make use of the mean (linear) thermal expansion coefficient (MTEC).[1] Some caution is needed in comparing MTEC values, since they may be dependent on the temperature range of the data if the behavior is not linear. Thermal expansion of the c cell parameter illustrates this influence. The value of c increases uniformly, although not linearly, with increasing temperature (Fig. 1); this is also true for calcite and magnesite. If one recognizes that the scale given for calcite in Figure 1 is different from those for dolomite and magnesite, it is easily seen that expansion of c in dolomite is more similar to that in magnesite than in calcite. Accordingly, MTEC values for dolomite (given in Table 7) and for calcite and magnesite (taken from Markgraf and Reeder) reflect this: MTEC $\times 10^6 = 25.8$, 22.9, and 32.3°C^{-1} for dolomite, magnesite, and calcite, respectively. However, such a comparison is not strictly appropriate since the data for magnesite extend only to 500°C, whereas those for dolomite extend to 700°C and those for calcite

[1] $\text{MTEC} = \frac{1}{X_{24}} \cdot \left(\frac{X_T - X_{24}}{T - 24}\right)$, where X_{24} is the room-temperature value of the parameter in question; the term in parentheses is the slope (determined in this paper from a linear least-squares regression of X vs. T).

Table 2. Unit-cell parameters for dolomite at several temperatures

T(°C)	a (Å)	c (Å)	V (Å^3)
24	4.8069(9)	16.002(1)	320.2(1)
200	4.8104(9)	16.055(1)	321.7(1)
400	4.8162(7)	16.132(1)	324.1(1)
600	4.8228(7)	16.227(1)	326.9(1)
700	4.827(1)	16.279(1)	328.4(2)

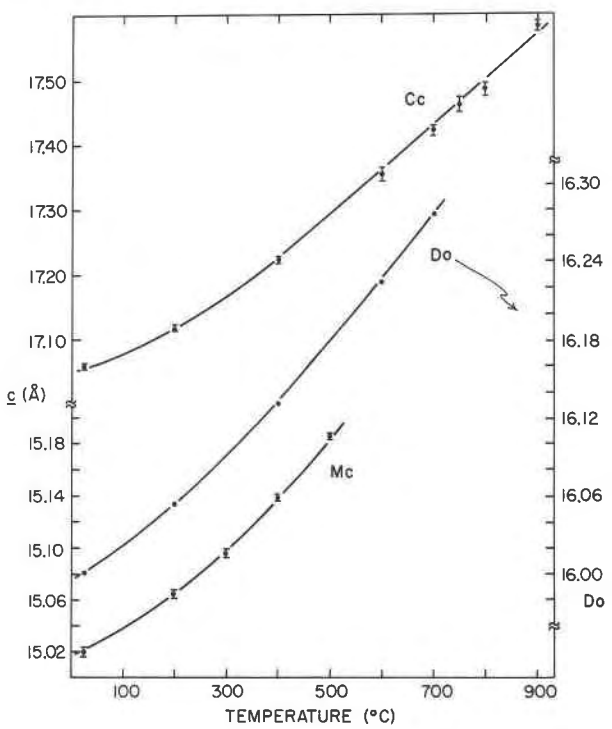

Fig. 1. Variation of c unit-cell parameter with temperature for dolomite (this study) and calcite and magnesite (from Markgraf and Reeder, 1985). The scale for dolomite is given on the right side of the diagram and is equivalent to the scale given for magnesite; the scale for calcite is different. (Error bars represent two standard deviations of the parameter; if no bars are given, the error is contained within the area of the symbol. Abbreviations: Do = dolomite; Cc = calcite; Mc = magnesite. These conventions are followed in all subsequent figures.)

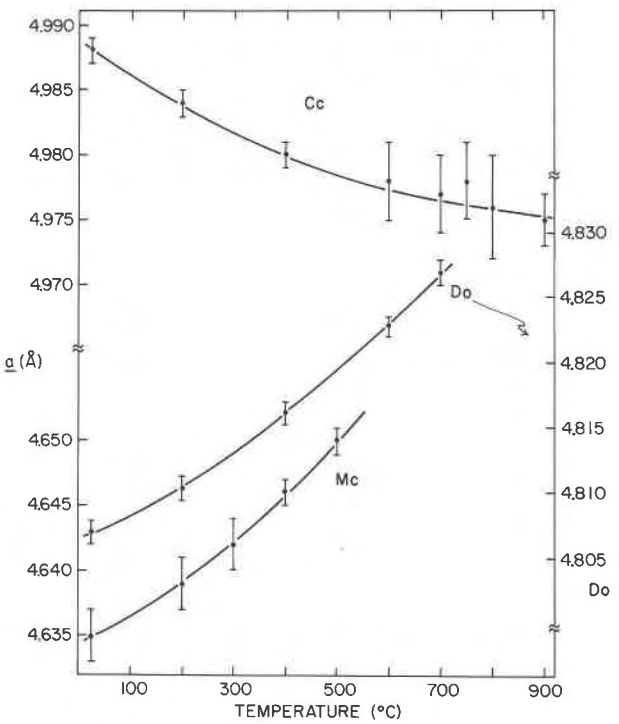

Fig. 2. Variation of a unit-cell parameter with temperature for dolomite (this study) and calcite and magnesite (Markgraf and Reeder, 1985). The scale for dolomite, given on the right side of the diagram, is the same as for calcite and magnesite.

up to 900°C. If the temperature range over which MTEC values are calculated is limited so as to be approximately comparable—that is, 24–500°C for magnesite and dolomite[2] and 24–700°C for calcite and dolomite—then the similarity for expansion along **c** with magnesite and the contrast with calcite are even further emphasized: MTEC $\times 10^6 = 22.9$ for both dolomite and magnesite, and 25.8 and 32.0 for dolomite and calcite, respectively. The difference in the calculated expansion coefficients resulting from the different temperature ranges of the data is often not very large, and for most purposes we will not need to use these "corrected" values for comparison. All MTEC values for calcite and magnesite are either taken from Table 10 of Markgraf and Reeder (1985) or are calculated from their data.

Expansion of a is also very nearly the same as in magnesite (Fig. 2). MTEC values compare quite closely: 6.2×10^{-6} for dolomite and 6.75×10^{-6}°C^{-1} for magnesite. Both differ markedly from calcite in which a contracts with increasing temperature. We also note that our expansion coefficients for both a and c—when corrected for the appropriate temperature range—agree closely with those determined by Bayer (1971) for dolomite using powder methods: 4.5×10^{-6} and 22.5×10^{-6}°C^{-1}, for a and c, respectively.

[2] For this purpose, the value for dolomite was interpolated from values at 400 and 600°C.

Thermal parameters

Anisotropic temperature factors and equivalent isotropic temperature factors from both conventional (anisotropic) and rigid-body refinements are reported in Table 3. At each temperature, agreement between results from the different refinement types is very good. In the rigid-body refinements, anisotropic temperature factors are calculated from the **T**, **L**, and **S** tensor coefficients and are not refined directly.

Figure 3 shows the variation of equivalent isotropic temperature factor, B_{eq}, with temperature; also shown are the corresponding values in calcite and magnesite. In general, the equivalent isotropic temperature factors for the atoms in dolomite represent an averaging of those in calcite and magnesite. B_{eq} values for carbon are approximately intermediate between those in calcite and magnesite. This is also generally true for oxygen; however, we note the rapid increase of B_{eq} for oxygen in calcite above 600°C, which is not suggested in the curve for dolomite. For Ca and Mg, the equivalent isotropic temperature factors in dolomite show less difference than in the single carbonates—that is, B_{eq} for Ca is less at all temperatures than in calcite, and B_{eq} for Mg is similarly greater than in magnesite. B_{eq} increases faster with temperature for Ca than for Mg, but not to the same extent as shown by Ca in calcite.

The slopes of B_{eq} vs. temperature for carbon and oxygen are very similar in dolomite. We also found a good correlation of this kind in magnesite; no such correlation was found in calcite.

Root-mean-square (RMS) amplitudes of the principal axes of vibrational ellipsoids calculated from anisotropic temperature factors are given in Table 4. The essential characteristics at room temperature have been discussed by Reeder and Wenk (1983). In the present study we observe no significant changes in shape or orientation of the ellipsoids over the temperature range studied. The ellipsoids for Ca and C remain spherical over the temperature range, and the Mg ellipsoid, which is only slightly prolate at room temperature, changes its shape very little. The oxygen ellipsoid is moderately anisotropic, but also does not change in shape over the temperature range. All magnitudes, of course, increase with temperature.

Interatomic distances

Libration of a rigid body causes an apparent decrease of interatomic distances within the rigid body (cf. Willis and Pryor, 1975). Markgraf and Reeder (1985) applied a correction for libration to C–O and O–O distances within the CO_3 group for calcite and magnesite; no other bond lengths were corrected. Of course, there may exist some type of correlated motion between other bonding atoms; however, there is no clear basis for applying any particular model. These same considerations apply in the present study, and we use the same procedures outlined in our previous study.

C–O bond lengths, corrected and uncorrected, are given in Table 5 and shown in Figure 4. As observed for calcite

Table 3. Positional and thermal parameters for dolomite at several temperatures

		Anisotropic refinement				Rigid-body refinement			
Atom	Parameter	24°C	200°C	400°C	600°C	24°C	200°C	400°C	600°C
Ca	β_{11}*	0.0111(2)	0.0158(2)	0.0225(2)	0.0303(2)	0.0110(2)	0.0157(2)	0.0225(2)	0.0303(2)
	β_{33}	0.00076(2)	0.00102(2)	0.00144(2)	0.00198(2)	0.00076(2)	0.00102(2)	0.00144(2)	0.00198(2)
	B**	0.77(1)	1.08(1)	1.54(1)	2.10(1)	0.77(1)	1.08(1)	1.54(1)	2.10(1)
Mg	β_{11}	0.0081(2)	0.0114(2)	0.0162(2)	0.0220(2)	0.0080(3)	0.0113(2)	0.0161(3)	0.0219(3)
	β_{33}	0.00074(2)	0.00100(2)	0.00143(3)	0.00193(3)	0.00073(3)	0.00100(3)	0.00143(3)	0.00194(3)
	B	0.63(1)	0.87(1)	1.25(1)	1.70(1)	0.62(1)	0.87(1)	1.24(1)	1.70(1)
C	z	0.24289(7)	0.24295(7)	0.24305(7)	0.24328(7)	0.24293(7)	0.24298(7)	0.24305(7)	0.24327(8)
	β_{11}	0.0098(4)	0.0126(4)	0.0173(4)	0.0220(4)	0.0084(3)	0.01132(3)	0.0158(3)	0.0207(3)
	β_{33}	0.00069(4)	0.00089(4)	0.00118(4)	0.00165(4)	0.00074(4)	0.00094(4)	0.00124(4)	0.00171(4)
	B	0.69(2)	0.89(2)	1.21(2)	1.60(2)	0.64(2)	0.85(2)	1.17(2)	1.57(2)
O	x	0.2480(1)	0.2470(1)	0.2457(1)	0.2447(2)	0.2479(1)	0.2469(1)	0.2456(2)	0.2446(2)
	y	-0.0354(1)	-0.0361(1)	-0.0368(1)	-0.0374(2)	-0.0355(1)	-0.0361(1)	-0.0369(2)	-0.0374(2)
	z	0.24393(3)	0.24401(3)	0.24416(3)	0.24430(4)	0.24392(3)	0.24400(3)	0.24415(4)	0.24430(4)
	β_{11}	0.0107(3)	0.0148(3)	0.0208(3)	0.0278(3)	0.0107(2)	0.0147(2)	0.0205(2)	0.0272(3)
	β_{22}	0.0148(3)	0.0205(3)	0.0284(3)	0.0380(4)	0.0148(3)	0.0205(3)	0.0284(4)	0.0379(4)
	β_{33}	0.00118(2)	0.00161(2)	0.00230(3)	0.00315(3)	0.00117(2)	0.00160(2)	0.00229(3)	0.00313(3)
	β_{12}	0.0083(2)	0.0117(2)	0.0162(3)	0.0217(3)	0.0080(2)	0.0112(2)	0.0155(2)	0.0208(2)
	β_{13}	-0.00059(5)	-0.00094(5)	-0.00139(6)	-0.00193(7)	-0.00057(5)	-0.00092(6)	-0.00136(6)	-0.00188(8)
	β_{23}	-0.00098(5)	-0.00146(6)	-0.00220(7)	-0.00293(8)	-0.00096(5)	-0.00144(6)	-0.00216(7)	-0.00288(8)
	B	0.93(1)	1.28(1)	1.82(2)	2.47(2)	0.94(1)	1.29(1)	1.83(1)	2.47(2)

* Anisotropic temperature factor of the form: $\exp[-\beta_{11}h^2+\beta_{22}k^2+\beta_{33}\ell^2+2\beta_{12}hk+2\beta_{13}h\ell+2\beta_{23}k\ell)]$

** Equivalent isotropic temperature factor of Hamilton (1959)

and magnesite, the uncorrected C–O bond length decreases with increasing temperature indicating correlated motion. The rate of decrease is roughly intermediate between that in calcite and magnesite. The libration-corrected bond length increases very slightly, but uniformly, over the temperature range studied and is nearly identical with that found in magnesite. The MTEC (4.1×10^{-6}°C^{-1}) agrees well with that for magnesite (3.4×10^{-6}°C^{-1}) and poorly with that for calcite (19.8×10^{-6}°C^{-1}).

Previous studies of dolomite (e.g., Beran and Zemann, 1977; Effenberger et al., 1981; Reeder and Wenk, 1983) have mentioned the aplanarity of the CO_3 group in dolomite; a very slight displacement of the carbon atom out of the plane of the oxygen atoms is observed—approximately 0.017(1) Å. Reeder and Wenk (1983) found that the average observed displacement decreases with increasing cation disorder. In the present study we find essentially no change in aplanarity with temperature.

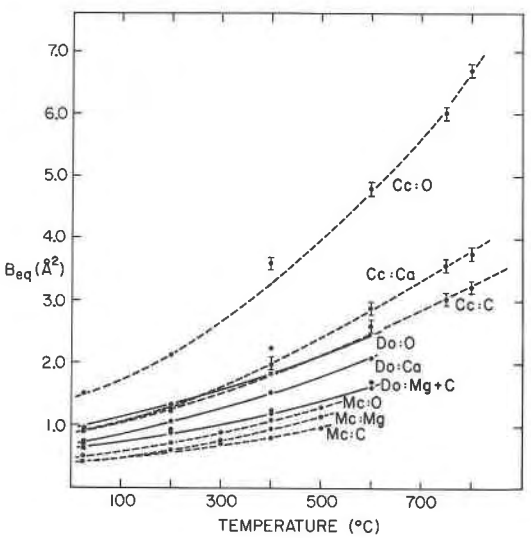

Fig. 3. Variation of the equivalent isotropic temperature factor, B_{eq}, with temperature for atoms in dolomite (solid lines) and calcite and magnesite (dashed lines). Abbreviations: Do:Ca = Ca in dolomite, etc.

Octahedral bond lengths are also given in Table 5. The variations of the Ca–O and Mg–O bond lengths with temperature are compared with those in calcite and magnesite in Figures 5 and 6. The longer Ca–O bond length in dolomite relative to that in calcite and the shorter Mg–O bond length relative to that in magnesite have been discussed elsewhere (e.g., Reeder, 1983). These differences in room-temperature bond lengths are *approximately* maintained over the temperature range studied. However, in dolomite the increase of Ca–O bond length is fairly linear with respect to temperature, whereas in calcite it is

Table 4. RMS amplitudes (Å) of the principal axes of thermal ellipsoids in dolomite

Atom	Axis	24°C	200°C	400°C	600°C
Ca	R_1	0.098(1)	0.118(1)	0.141(1)	0.164(1)
	R_3	0.100(1)	0.115(1)	0.138(1)	0.162(1)
Mg	R_1	0.085(1)	0.100(1)	0.120(1)	0.139(1)
	R_3	0.098(1)	0.115(1)	0.137(1)	0.161(1)
C	R_1	0.093(1)	0.105(1)	0.123(1)	0.139(1)
	R_3	0.095(2)	0.108(2)	0.125(2)	0.148(2)
O*	R_1	0.083(1)	0.097(1)	0.116(1)	0.133(1)
	R_2	0.104(1)	0.120(1)	0.141(1)	0.164(1)
	R_3	0.133(1)	0.158(1)	0.189(1)	0.221(1)

* Orientations of the principal axes for the oxygen ellipsoid are given in terms of three angles formed with the crystallographic axes $\underline{a}_1$, $\underline{a}_2$, and $\underline{c}$, respectively. For the refinement at 24°C these are: R_1--97(2), 129(2), and 91(2)°; R_2--98(2), 129(2), and 126(2)°; R_3 -- 86(1), 62(1), and 144(1)°. Values at other temperatures are not reported since no appreciable changes are observed. Orientations of principal axes for other atoms are constrained by symmetry; R_1 (=R_2) is normal to $\underline{c}$ and R_3 is parallel to $\underline{c}$.

Table 5. Selected interatomic distances (Å) for dolomite at several temperatures

Temp(°C)	M-O	O_1-O_2	O_1-O_6	O_1-O_2*	O_1-O_6*
CaO_6					
24	2.3816(5)	3.298(1)	3.437(1)	3.294(1)	3.436(1)
200	2.3881(6)	3.307(1)	3.446(1)	3.302(1)	3.444(1)
400	2.3966(6)	3.320(1)	3.457(1)	3.312(1)	3.455(1)
600	2.4056(6)	3.331(1)	3.471(1)	3.321(1)	3.467(1)
MgO_6					
24	2.0821(5)	2.902(1)	2.987(1)	2.896(1)	2.985(1)
200	2.0865(5)	2.904(1)	2.996(1)	2.896(1)	2.994(1)
400	2.0934(6)	2.908(1)	3.012(1)	2.896(1)	3.008(1)
600	2.1018(6)	2.914(1)	3.030(1)	2.896(1)	3.024(1)
	C-O	C-O**	O-O	O-O**	
CO_3					
24	1.2858(5)	1.2900(7)	2.227(1)	2.234(1)	
200	1.2836(6)	1.2900(7)	2.223(1)	2.234(1)	
400	1.2815(6)	1.2911(7)	2.219(1)	2.236(1)	
600	1.2798(6)	1.2930(8)	2.217(1)	2.239(1)	

* Distance calculated from oxygen positions that have been corrected for libration, see discussion in text.
** Corrected for libration.

not. Over the temperature range 24–600°C, the MTEC is noticeably higher in dolomite (17.6×10^{-6}°C^{-1}) than in calcite (12.1×10^{-6}°C^{-1}); only above approximately 600°C does the rate of increase of the Ca–O bond length approach that in dolomite. This difference in expansion may reflect a corresponding difference in bond strength in the different structures, with the shorter, stronger bond (in calcite) expanding less rapidly. However, a similar effect is not observed with the MgO_6 octahedra, as MTECs for the Mg–O bond are comparable in dolomite and magnesite.

Thus, volume expansion of the CaO_6 octahedron in dolomite (Table 6) is more rapid than in calcite—especially so over the temperature range 24–600°C—but that for the MgO_6 octahedron is similar to that in magnesite. Relative to one another, the octahedra in dolomite expand at a fairly similar rate, the Ca octahedron expanding slightly faster. We note, however, different trends of polyhedral distortion. Quadratic elongation values (Robinson et al., 1971) given in Table 6 reveal no change in distortion for the CaO_6 octahedron with temperature, but do show a small, uniform increase for the MgO_6 octahedron. This contrasts with distortion trends in calcite and magnesite, where CaO_6 shows a marked increase with temperature, but MgO_6 shows essentially no change.

The basis for these trends in polyhedral distortion is found in the thermal expansions of the O–O interatomic distances within the octahedra. If we compare MTEC values (Table 7) for the basal edge (O_1–O_2) and the lateral edge (O_1–O_6),[3] we find that they are essentially identical

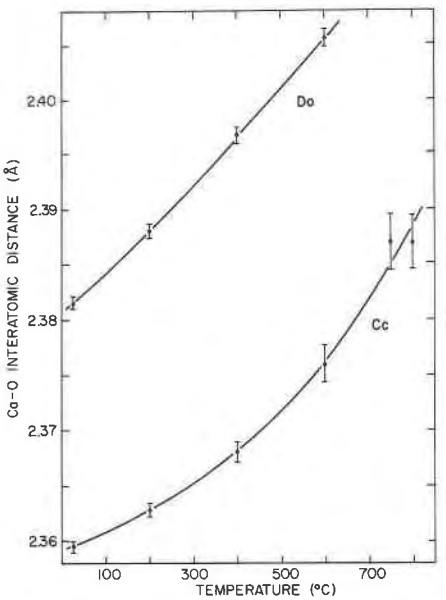

Fig. 5. Variation of Ca–O interatomic distance with temperature in dolomite (this study) and calcite (Markgraf and Reeder, 1985).

[3] Oxygen atoms are labeled according to the scheme given by Reeder (1983).

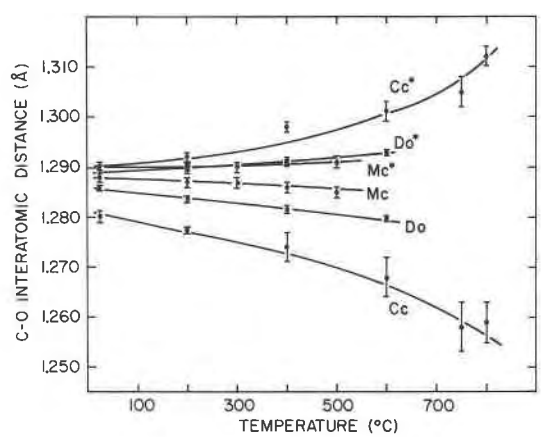

Fig. 4. Variation of C–O interatomic distance in dolomite (this study) and calcite and magnesite (Markgraf and Reeder, 1985). The asterisk denotes values corrected for rigid-body libration.

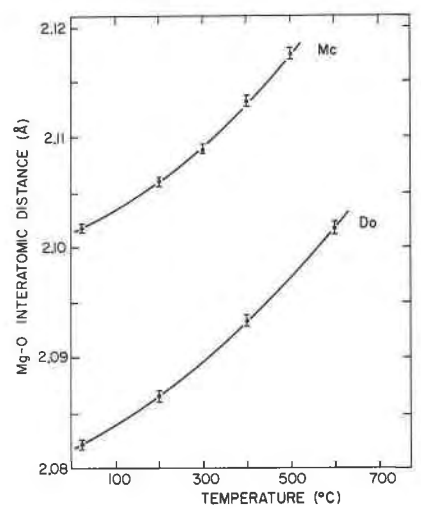

Fig. 6. Variation of Mg–O interatomic distance with temperature in dolomite (this study) and magnesite (Markgraf and Reeder, 1985).

Table 6. Octahedral volumes and quadratic elongation (QE) for dolomite at several temperatures

TEMP(°C)	V(Å3)	QE
CaO_6		
24	17.96(1)	1.0017(1)
200	18.12(1)	1.0017(1)
400	18.31(1)	1.0016(1)
600	18.51(1)	1.0016(1)
MTEC*	53.2×10^{-6} °C^{-1}	
MgO_6		
24	12.02(1)	1.0008(2)
200	12.09(1)	1.0010(2)
400	12.21(1)	1.0012(2)
600	12.35(1)	1.0015(2)
MTEC*	48.1×10^{-6} °C^{-1}	

* Mean thermal expansion coefficient for octahedral volume.

Table 7. Mean (linear) thermal expansion coefficients* for selected distances in dolomite

Parameter	MTEC$\times 10^6$(°C^{-1})	T Interval (°C)
a	6.2	24-700
c	25.8	"
Ca-O	17.6	24-600
Mg-O	16.5	"
C-O	-8.1	"
C-O**	4.1	"
O_1-O_2 (CaO_6)	17.6	"
O_1-O_6 (CaO_6)	17.1	"
O_1-O_2 (MgO_6)	7.2	"
O_1-O_6 (MgO_6)	25.3	"

* See text
** Corrected for libration

within the CaO_6 octahedron of dolomite—17.6×10^{-6} (O_1–O_2) and 17.1×10^{-6}°C^{-1} (O_1–O_6). For the MgO_6 octahedron they are substantially different—7.2×10^{-6} (O_1–O_2) and 25.3×10^{-6}°C^{-1} (O_1–O_6)—yielding the increasing quadratic elongation. These relationships again contrast sharply with those for the respective single carbonates, where MTECs are 5.7×10^{-6} (O_1–O_2) and 25.1×10^{-6}°C^{-1} (O_1–O_6) for calcite and 11.5×10^{-6} (O_1–O_2) and 19.3×10^{-6}°C^{-1} (O_1–O_6) for magnesite. Thus, the strong anisotropy of expansion of the CaO_6 octahedron in calcite is not present in dolomite, yet the moderate expansion anisotropy of MgO_6 in magnesite is increased in dolomite.

Rigid-body motions

Independent coefficients of the T, L, and S tensors from the rigid-body refinements are reported in Table 8. Their physical significance is discussed by Finger (1975), by Markgraf and Reeder (1985), and, in a more general sense, by Willis and Pryor (1975). Owing to the lower point symmetry of the CO_3 group in dolomite (3) as compared to calcite (32), one additional coefficient (S_{12}) must be refined; in calcite S_{12} is constrained by symmetry to be zero. It is interesting to note that at all temperatures, S_{12} refines to a value of zero (within estimated standard errors). Thus, the screw-coupling is essentially no different than in calcite or magnesite, except in relative magnitude.

In view of the results on thermal parameters relative to calcite and magnesite, it is not surprising to find that rigid-body motion parameters for dolomite are also generally intermediate between those for the respective single carbonates. Examples are shown in Figures 7 and 8 for T_{11} and L_{33}. For both independent T tensor coefficients, the rate of increase with temperature is fastest for calcite. Rates of increase for dolomite and magnesite tend to be roughly similar. Libration tensor coefficients emphasize even more the similarity of dolomite and magnesite and the "uniqueness" of calcite. In Figure 8, the L_{33} libration parameter for calcite increases at a markedly higher rate than for either magnesite or dolomite. The S_{11} screw-coupling parameter is fairly small in dolomite, again more similar to that in magnesite than in calcite where it is large.

In our earlier study of calcite and magnesite, we observed different trends for the libration parameters between the two minerals—for calcite $L_{33} > L_{11}$ and for magnesite $L_{11} > L_{33}$. In dolomite we find that L_{11} and L_{33} are fairly similar at all temperatures, with L_{11} becoming slightly larger at higher temperatures. The trend $T_{33} > T_{11}$ found in both calcite and magnesite is also true for dolomite.

Although the amplitudes of libration of the CO_3 group in these minerals may be small in comparison to some organic molecules, they are by no means insignificant. RMS amplitudes of libration at room temperature range between 2 and 5° for calcite, magnesite, and dolomite. At 600°C, amplitudes are greater than 6° in dolomite, and at 800°C they are over 13° in calcite!

Discussion

The carbonate group

Our comparison of thermal parameters and residuals indicates that the rigid-body model gives an equally sat-

Table 8. Rigid-body motion parameters for the CO_3 group in dolomite at several temperatures

TEMP (°C)	T_{11} (Å^2)	T_{33} (Å^2)	L_{11} (Rad^2)	L_{33} (Rad^2)	S_{11} (Rad-Å)	S_{12} (Rad-Å)
24	0.0074(2)	0.0096(5)	0.0033(3)	0.0034(2)	0.0008(1)	0.0001(1)
200	0.0099(2)	0.0123(5)	0.0052(3)	0.0049(2)	0.0013(1)	0.0001(1)
400	0.0139(3)	0.0164(5)	0.0084(3)	0.0068(2)	0.0019(1)	0.0000(1)
600	0.0183(3)	0.0229(5)	0.0115(4)	0.0094(3)	0.0026(1)	0.0002(2)

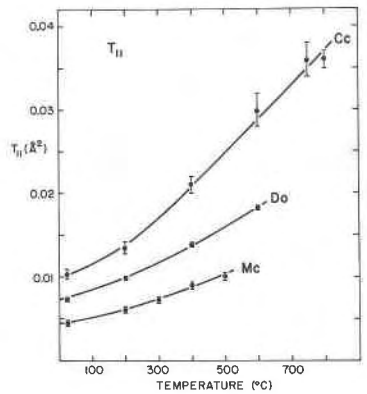

Fig. 7. Variation of T_{11} rigid-body translation coefficient with temperature for the CO_3 group in dolomite (this study) and calcite and magnesite (Markgraf and Reeder, 1985).

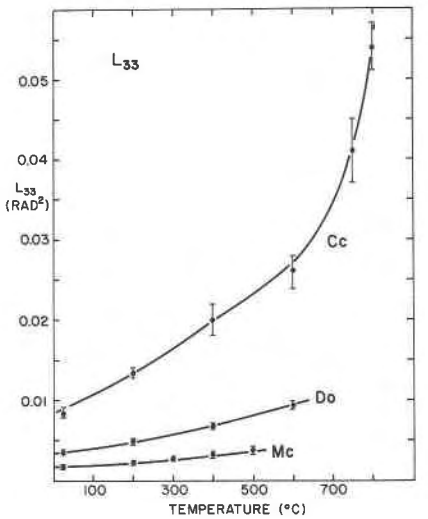

Fig. 8. Variation of L_{33} rigid-body libration coefficient with temperature for the CO_3 group in dolomite (this study) and calcite and magnesite (Markgraf and Reeder, 1985).

isfactory explanation for the data as the conventional anisotropic model. As in our previous study of calcite and magnesite, we believe that this suggests the validity of the rigid-body model over the temperature range studied. Rosenfield et al. (1978) have devised a simple test for rigid-body vibrations that—as the authors point out—is a necessary, but by no means sufficient, condition for proper application of the model. For all pairs of atoms within a molecular unit, the difference between the individual mean square displacement amplitudes should be approximately zero along the direction of the bond. We have calculated these differences from the refined anisotropic temperature factors for directions along the C–O and O–O bonds within a CO_3 group. They are indeed approximately zero within estimated errors, further strengthening our premise.

The average motions of the CO_3 group in dolomite are intermediate between those in calcite and magnesite, being dominated neither by the rotary oscillation around the three fold axis combined with strong screw-coupling as in calcite nor the tilting out of the basal plane as in magnesite. Amplitudes of rigid-body motions, while also intermediate between those of the respective single carbonates, favor those in magnesite. This is especially true for the libration and screw-coupling parameters. The difference in rigid-body motion reflects the net cation coordination of the CO_3 group. The shorter, stronger Mg–O bond has the effect of restricting the motion of the individual oxygens—relative to that in calcite—and hence the motions of the CO_3 group are also less. In magnesite the amplitudes are even less.

Accounting for the bond-length correction due to libration, mean linear thermal expansion for the C–O interatomic distance in dolomite (4.1×10^{-6}°C^{-1}) is virtually the same as in magnesite (3.4×10^{-6}°C^{-1}). These values agree closely with the correlations between mean polyhedral thermal expansion and Pauling bond strength, which were found by Hazen and Prewitt (1977) and Hazen and Finger (1982, p. 127). Uncorrected values deviate significantly from this relationship. Expansion of the CO_3 group in calcite is anomalous, deviating significantly from the observed trend.

For calcite, we interpreted the extremely rapid increase of the L_{33} libration parameter above 600°C as premonitory behavior consistent with the onset of rotational disorder at some higher temperature (also see discussion by Carlson, 1983). The dominant motion was found to be a rotary oscillation around the threefold axis, which is a motion analogous to that for rotational disorder. On the other hand, in magnesite, libration parameters indicated a tilting of the CO_3 group out of the basal plane as the dominant motion; the amplitudes are also much less than in calcite. As we have pointed out, the average motion of the CO_3 group in dolomite is dominated by neither character, but is fairly low in amplitude like that in magnesite. If the relatively large amplitude libration in calcite *is* a precursor to rotational disorder, then it seems very unlikely that such disordering would ever occur in dolomite or magnesite, unless at a significantly higher temperature than in calcite.

Thermal expansion

Unit-cell thermal expansion in dolomite, as noted earlier, is similar to that in magnesite, differing considerably from that in calcite. Since the structural linkage in dolomite is essentially identical to that in calcite, we may expect the same mechanisms of thermal expansion to be operative—that is, expansion of the polyhedra and opening of the structure by tilting of polyhedral elements. The latter is actually a very minor influence since the rigid CO_3 groups prevent any appreciable tilting of the octahedra relative to one another. Nor does the orientation of the CO_3 group change significantly at higher temperatures. At room temperature the displacement of the oxygen atoms off the a axes corresponds to a 6.5° rotation of the CO_3 group from the position in calcite. This rotation angle changes less than 0.5° at 600°C, indicating that tilting of polyhedral elements is minimal. The major difference

to keep in mind with dolomite is that each octahedron shares corners with *unlike* octahedra in adjacent layers; no corner sharing between like octahedra occurs. Thus, expansion of an octahedron within the basal plane is constrained by that of the unlike octahedra (and the CO_3 groups) sharing its corners.

Expansion along **c** is the net effect of expansion of the CaO_6 and MgO_6 octahedra. Judging from their behavior in the single carbonates, one would expect expansion of the CaO_6 octahedra to be more important. This is not the case, however, as shown by the MTECs for the lateral edges of the CaO_6 and MgO_6 octahedra—17.1×10^{-6} and 25.3×10^{-6}°C^{-1}, respectively. The stronger influence of the MgO_6 octahedra may explain the similar expansion along **c** of dolomite relative to magnesite. In addition, quadratic elongation does not increase with temperature for CaO_6, as it did in calcite. The lack of expansion anisotropy of the CaO_6 octahedra, contrary to that in calcite, must reflect the corner sharing with MgO_6 octahedra in adjacent layers.

Expansion along **a** is controlled by expansion of the basal octahedral edge lengths and by the magnitude of libration of the CO_3 group. Expansion of the C–O bond length is relatively unimportant. Markgraf and Reeder (1985) combined these influences in a hypothetical interatomic distance to explain expansion in calcite and magnesite. This distance corresponds to the basal octahedral edge length (O_1–O_2), but is calculated using coordinates of oxygen that have been corrected for libration *within* the individual CO_3 groups.[4] These "corrected" interatomic distances are given in Table 5. We note that the corrected basal edge length (O_1–O_2*) increases with temperature in the CaO_6 octahedra but does not change in MgO_6. In the absence of large libration parameters (relative to calcite), expansion of the CaO_6 octahedra has the predominant effect on expansion of the *a* cell parameter. The cause for the marked difference in character of expansion anisotropy of the CaO_6 octahedron, and to a lesser extent the MgO_6 octahedron, is not entirely clear. Within {0001}, expansion of the corner-linked basal-edge lengths of the CaO_6 and MgO_6 octahedra are constrained by one another and, of course, also by the rigid CO_3 groups. A possible explanation is that the inherently greater expansivity of the CaO_6 octahedron allows it to expand *even more* in this direction against the more slowly expanding MgO_6. Thus, the relative difference in bond strengths within these octahedra would be the important factor. Given this greater expansion of the CaO_6 octahedron parallel to {0001}, its relatively subdued expansion parallel to **c** is not unexpected. The reverse arguments can be applied to the MgO_6 octahedron to explain its greater anisotropy of expansion compared with that in magnesite. The fact that the MTEC for expansion of *a* is so similar to that of magnesite is largely a result of the low amplitude of libration of the CO_3 group.

Thus, expansion of the octahedra is the major factor responsible for unit-cell thermal expansion. This is further demonstrated by the almost negligible change with temperature of the proportion of the unit-cell volume occupied by the cation octahedra—28.1% at 24°C and 28.3% at 600°C. Not surprisingly, expansion of the CO_3 groups is relatively unimportant.

[4] These O_1–O_2 distances are themselves not corrected for libration, since no rigid-body correlation exists *between* CO_3 groups.

Acknowledgments

We would like to thank K. J. Baldwin and D. K. Swanson for providing help in the laboratory and C. T. Prewitt for stimulating discussions. T. Yamanaka's thorough review improved the manuscript and helped to clarify several aspects. Financial support was provided by NSF Grants EAR 8106629 and EAR 8416795 to RJR.

References

Barber, D.J., Heard, H.C., and Wenk, H.-R. (1981) Deformation of dolomite single crystals from 20–800°C. Physics and Chemistry of Minerals, 7, 271–286.

Bayer, G. (1971) Thermal expansion anisotropy of dolomite-type borates $Me^{2+}Me^{4+}B_2O_6$. Zeitschrift für Kristallographie, 133, 85–90.

Becker, P.J., and Coppens, P. (1975) Extinction within the limit of validity of the Darwin transfer equations. III. Nonspherical crystals and anisotropy of extinction. Acta Crystallographica, A31, 417–425.

Beran, A., and Zemann, J. (1977) Refinement and comparison of the crystal structures of a dolomite and of an Fe-rich ankerite. Tschermaks Mineralogische und Petrographische Mitteilungen, 24, 279–286.

Brown, G.E., Sueno, S., and Prewitt, C.T. (1973) A new single-crystal heater for the precession camera and the four-circle diffractometer. American Mineralogist, 58, 698–704.

Carlson, W.D. (1983) The polymorphs of $CaCO_3$ and the aragonite-calcite transformation. In R.J. Reeder, Ed. Carbonates: Mineralogy and chemistry. Mineralogical Society of America Reviews in Mineralogy, 11, 191–225.

Effenberger, H., Mereiter, K., and Zemann, J. (1981) Crystal structure refinements of magnesite, calcite, rhodochrosite, siderite, smithsonite, and dolomite with discussion of some aspects of the stereochemistry of calcite-type carbonates. Zeitschrift für Kristallographie, 156, 233–243.

Finger, L.W. (1975) Least-squares refinement of the rigid-body motion parameters of CO_3 in calcite and magnesite and correlation with lattice vibrations. Carnegie Institution of Washington Year Book 74, 572–575.

Finger, L.W., and Prince, E. (1975) A system of FORTRAN IV computer programs for crystal structure computations. U.S. National Bureau of Standards Technical Note 854.

Graf, D.L., and Goldsmith, J.R. (1955) Dolomite-magnesian calcite relations at elevated temperatures and CO_2 pressures. Geochimica et Cosmochimica Acta, 7, 109–128.

Hamilton, W.C. (1959) On the isotropic temperature factor equivalent to a given anisotropic temperature factor. Acta Crystallographica, 12, 609–610.

Hazen, R.M., and Finger, L.W. (1982) Comparative crystal chemistry. John Wiley, New York.

Hazen, R.M., and Prewitt, C.T. (1977) Effects of temperature and pressure on interatomic distances in oxygen-based minerals. American Mineralogist, 62, 309–315.

Higgs, D.V., and Handin, J.W. (1959) Experimental deformation of dolomite single crystals. Geological Society of America Bulletin, 70, 245–278.

Ibers, J.A., and Hamilton, W.C., Eds. (1974) International tables for X-ray crystallography, volume 4. Revised and supplementary tables. Kynoch Press, Birmingham.

Markgraf, S.A., and Reeder, R.J. (1985) High-temperature structure refinements of calcite and magnesite. American Mineralogist, 70, 590–600.

Reeder, R.J. (1983) Crystal chemistry of the rhombohedral carbonates. In R.J. Reeder, Ed. Carbonates: Mineralogy and chemistry. Mineralogical Society of America Reviews in Mineralogy, 11, 1–47.

Reeder, R.J., and Nakajima, Y. (1982) The nature of ordering and ordering defects in dolomite. Physics and Chemistry of Minerals, 8, 29–35.

Reeder, R.J., and Sheppard, C.E. (1984) Variation of lattice parameters in some sedimentary dolomites. American Mineralogist, 69, 520–527.

Reeder, R.J., and Wenk, H.-R. (1983) Structure refinements of some thermally disordered dolomites. American Mineralogist, 68, 769–776.

Robinson, K., Gibbs, G.V., and Ribbe, P.H. (1971) Quadratic elongation: A quantitative measure of distortion in coordination polyhedra. Science, 172, 567–570.

Rosenfield, R.E., Trueblood, K.N., and Dunitz, J.D. (1978) A test for rigid-body vibrations, based on Hirshfeld's 'rigid-bond' postulate. Acta Crystallographica, A34, 828–829.

Schomaker, V., and Trueblood, K.N. (1968) On the rigid-body motion of molecules in crystals. Acta Crystallographica, B24, 63–76.

Willis, B.T.M., and Pryor, A.W. (1975) Thermal vibrations in crystallography. Cambridge University Press.

Zucker, U.H., Perenthaler, E., Kuhs, W.F., Bachmann, R., and Schulz, H. (1983) PROMETHEUS. A program system for investigation of anharmonic thermal vibrations in crystals. Journal of Applied Crystallography, 16, 358.

MANUSCRIPT RECEIVED JULY 15, 1985
MANUSCRIPT ACCEPTED JANUARY 17, 1986